

Content from this work may be used under the terms of the CC BY 3.0 licence (© 2015). Any distribution of this work must maintain attribution to the author(s), title of the work, publisher, and DOI.

# OPTIMIZATION OF ORBITS, SRF ACCELERATION, AND FOCUSING LATTICE FOR A STRONG-FOCUSING CYCLOTRON

K. Melconian<sup>#</sup>, J. Gerity, J. Kellams, P. M. McIntyre, A. Sattarov, S. Assadi, Texas A&M University, College Station, TX 77845 USA

N. Pogue, Paul Scherrer Institute, Villigen, Switzerland

## Abstract

The strong-focusing cyclotron is an isochronous sector cyclotron designed to accelerate >10 mA CW beams of protons and ions up to >500 MeV/u with low loss and high efficiency. Superconducting RF cavities are used to provide enough energy gain per turn to fully separate orbits, and arc-shaped beam transport channels in the sector dipole apertures provide strong focusing of all orbits. A design methodology is being developed to optimize the sector dipoles, the focal lattice, and the SRF cavities so that betatron tunes can be locked to favorable operating point. Provision is made for correction of dispersion and chromaticity. The methodology will provide a framework on which we can then proceed to study and optimize the nonlinear beam dynamics for high-current transport.

## INTRODUCTION

The Accelerator Research Laboratory at Texas A&M University is developing a strong-focusing cyclotron (SFC) for applications requiring high-current beams or micro-emittance beams [1]. Applications include an 800 MeV, >10 mA proton driver for accelerator-driven fission to destroy the transuranics and burn to completion the depleted uranium in spent nuclear fuel [2], a 100 MeV, >10 mA p/α driver for cost-effective production of medical isotopes [3], and a 100 MeV spallation driver for fast neutron damage studies [4].

A 100 MeV SFC is shown in cutaway in Figure 1. It contains 4 superconducting RF cavities [5] that provide enough energy gain to fully separate successive orbits ( $\Delta r > 6$  cm). Each sector dipole consists of a warm-iron flux return with a pair of cold-iron flux plates suspended in the mid-plane gap to define the magnetic field  $B(r)$  required for isochronicity [6]. An array of arc-shaped beam transport channels (BTCs, shown as blue in Figure 1) are located in the aperture between the flux plates, each aligned to define the equilibrium trajectory for one orbit in that sector [7]. Each BTC contains an F-D quadrupole doublet and a dipole correction winding, all fabricated as wire-wound superferric windings on a square beam channel. 80% of the 6 cm orbit spacing is available for particle trajectories.

In a previous study [8], we made a first design for a 100 MeV SFC and simulated several aspects of single-bunch dynamics of high-current proton bunches. That study validated that the SFC should be capable of accelerating >10 mA of CW beam without limitations from the effects that are known to limit beam current at PSI.

<sup>#</sup>This work supported by the George and Cynthia Mitchell Foundation.  
<sup>#</sup>KarieMelconian@tamu.edu

The SFC design builds upon an earlier design for a separated-orbit cyclotron, TRITRON [9], which also used SRF cavities and quadrupole channels. Although TRITRON successfully demonstrated transport of beam through several orbits, the orbit separation was small (10 mm) and the fraction of aperture with usable field quality for orbits was ~40%. In order to avoid this limitation, the beam transport channels in the SFC have been designed with > 6 cm orbit separation and 4 cm good-field aperture in each BTC.

Table 1: Main Parameters of the SFC Design

Proton energy (inj/ext)	13/100	MeV
RF frequency	117	MHz
Orbit radius (inj/ext)		m
Dipole field (inj/ext)	0.60/0.45	T

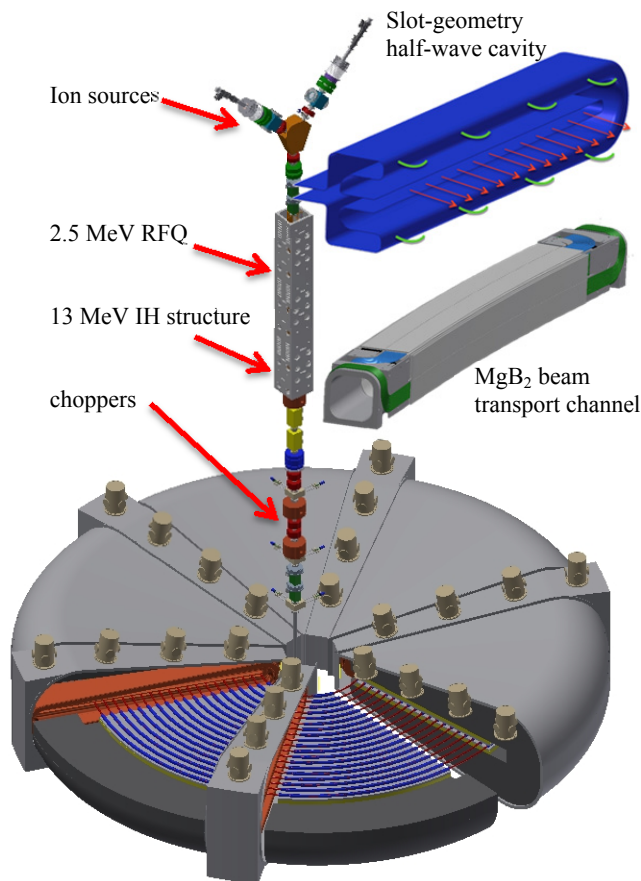


Figure 1: 100 MeV SFC, with cutaway to show SRF cavities and beam transport channels.

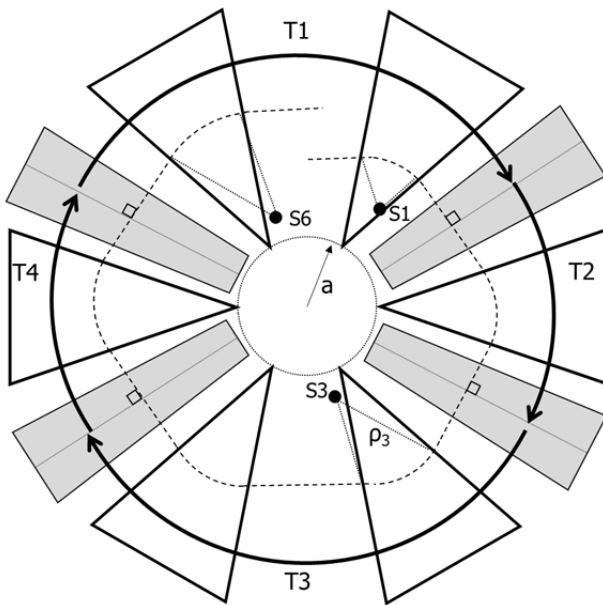


Figure 2: Geometric layout and spiral for optimizing isochronous orbits.

The main components of the SFC are shown in cutaway view in Figure 1. It also shows a detail of the slot-geometry half-wave SRF cavity, which is driven by rows of input couplers along its top and bottom lobes, and of the beam transport channel, which provides up to 6 T/m gradient in a 4cm x 4cm clear aperture.

In what follows, we present the methodology used to design the geometry, the orbits, and the linear optics of a 100 MeV SFC:

- the sector dipoles and their field profile;
- the optimization a pattern of isochronous orbits to maintain  $\sim$ uniform orbit separation and provide for normal incidence to SRF cavities;
- energy gains on the orbit traversals of each cavity that is consistent with the field design of the cavity;
- settings for the F/D quad doublets to provide good phase advance/cell and constant betatron tunes.

## ISOCHRONOUS ORBITS

For cyclotrons, the reference orbit and corresponding magnet parameters are often calculated based on a series of closed orbits, assuming no energy gain through one turn of the machine. Although the actual orbit is a spiral, this approximation works because the actual path of the beam is not constrained within the cyclotron. In the TAMU machine, the trajectory of all orbits is defined by the placement of the arc-shaped BTCs in each sector. It is therefore necessary to meticulously define that geometry to satisfy all constraints for optimal operation. A geometric approach was used to obtain a spiral trajectory that reflects the pattern of energy gains from the SRF cavities, satisfies isochronicity on all orbits, maintains a minimum spacing between successive orbits to accommodate the BTCs, and enters each SRF cavity perpendicular to the

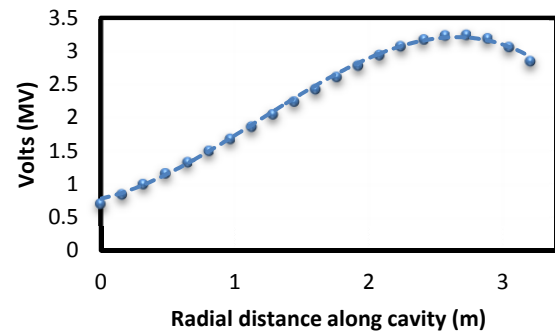


Figure 3: Energy gain in each SRF cavity voltage vs. orbit radius.

cavity axis so that the bunch is not deflected by the accelerating fields.

Figure 2 shows the geometry of the sector dipoles that was used to calculate the dipole field distribution and the spiral trajectory. Each sector dipole has an overall geometry that is an isosceles triangle with a vertex angle  $\theta < 60^\circ$ , and the vertices of the 6 sectors are positioned symmetrically on a circle of radius  $a$ . The sectors are oriented symmetrically so that their sides make equal angles to neighboring sectors, and the offset radius is chosen to provide sufficient gap to accommodate the SRF cavities. The vertex angle  $\theta = 52.42^\circ$  is chosen so that the margin between the dipole edge and the boundary of the neighboring tapered cavity [5] increases with radius and can accommodate tilting of each cavity to provide an extra degree of freedom in attaining isochronicity and orthogonal paths at cavity entrance.

A set of 52 parametric equations were developed to describe the path through the sectors and RF cavities for each spiral orbit, based on the above sector geometry, parameters that carry from the previous orbit, and on parameters to be optimized. The carry-over parameters are the starting radius, the starting time with respect to a global RF clock, the starting energy, and the angle of approach to the first sector. Those parameters for the first orbit are used to characterize the injection to the SFC.

A set of global cavity parameters are required to complete the definition of the SFC geometry: the tilt, the radial offset, and the RF amplitude  $V_n$  and global phase  $\varphi_n$  for each of the 4 cavities.

A Mathematica optimization script Global Optimization 10 [10] is used to optimize the choice of the global parameters and also of two additional independent parameters that fully define each orbit in turn: the centers of curvature S3 and S6 for the bending trajectory through sectors 3 and 6.

### Optimizing the Injection Orbit

Optimization begins with the injection orbit ( $m=0$  for the indexing of parameters). The script cycles through a bounded range of values for the global cavity parameters and the values of S3 and S6 to give a minimum error in the transit times T1-T4 through the four segments of the

Content from this work may be used under the terms of the CC BY 3.0 licence (© 2015). Any distribution of this work must maintain attribution to the author(s), title of the work, publisher, and DOI.

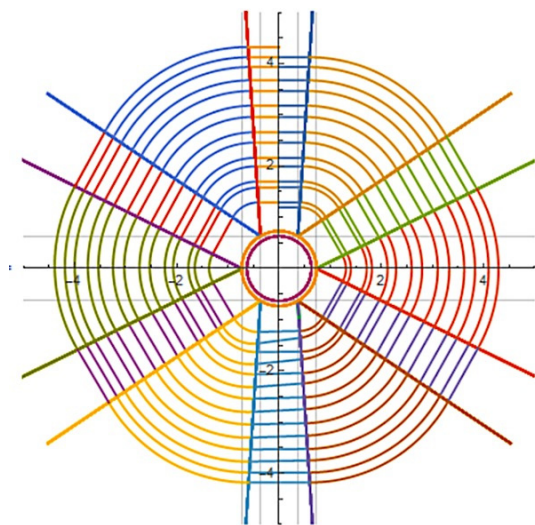


Figure 4: Spiral orbits after optimization for isochronicity.

orbit connecting the RF cavities (Figure 2), and also to maintain the spacing between successive orbits to be at least 6 cm. For the arc trajectory through the  $n$ th sector in the orbit, the entry location and the location of the center of curvature determine the radius of curvature (e.g.  $\rho_{03}$  for sector 3 in Figure 2), and together with the energy at that sector it determines the dipole field  $B_{0n}$  for the  $m$ th orbit following the  $n$ th sector.

The range of allowed values for global cavity parameters is bounded to avoid unrealistic solutions such as cavities overlapping sectors. The path lengths in each sector, in the gap between sectors, and in the cavity are calculated based on the initial values of the global parameters, the above trajectory, and the energy gained in each cavity. The time is then obtained by dividing each path segment by its corresponding velocity. The energy gain is based on the phase  $\omega T_n - \varphi_n$  and the energy at the time of arrival at the cavity, and the RF amplitude  $V_{0n}$  appropriate for the radius at the entrance of the  $n$ th cavity (Figure 3):

$$\Delta E_{0n} \approx qV_{0n} \left[ 2\beta c \frac{\sin\left(\frac{\omega_{RF}L_{0n}}{2\beta c}\right)}{\omega_{RF}L_{0n}} \right] \cos(\omega T_{0n} - \varphi_n) \quad (1)$$

The bracketed expression is the transit time factor across the accelerating gap  $L_n$  (which increases with radius in the tapered geometry of the SRF cavities).

### Optimizing Subsequent Orbits

For each subsequent orbit the script uses the values for global cavity parameters determined for the injection orbit and optimizes the values of S3 and S6 to give a minimum error for the transit times T1 and T3 (the other two transit times are constrained by the global parameters). The entire geometry of each orbit is thereby determined, including the values  $B_{mn}$  of the dipole field in each sector and the energy gain  $\Delta E_{mn}$  at each cavity.

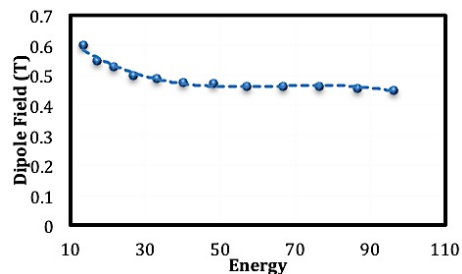


Figure 5: Profile of the required  $B(r)$  in one of the sectors.

The optimization script cycles through all orbits in turn until the energy reaches the desired extraction energy. If

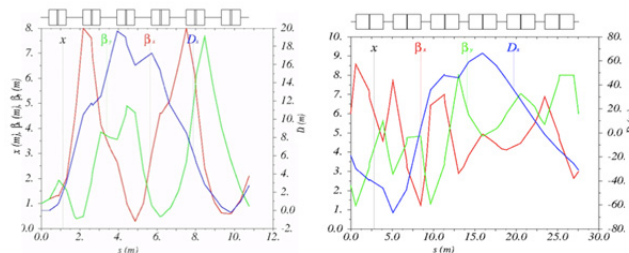


Figure 6: MAD lattice for the first and last orbits.

at any stage the script fails to reach a minimization that satisfies all conditions (isochronicity, beam spacing) the initial values of the global parameters are iterated and the process is repeated until a solution is found. By this procedure the script has been successful in defining a trajectory whose isochronicity is within 1% of a defined value throughout all orbits. Figure 4 shows an example outcome from the optimization.

## BEAM OPTICS

MADX [11] file was generated using the geometry, magnetic fields, and energy gains from the above optimization. Each of the six sectors is split into three sections, a combined-function focusing (F) section, a sector bend (no gradient), and a combined-function defocusing (D) section. The SBEND feature in MADX is used to optimize the F and D gradients to lock the betatron tunes to a desired operating point for all orbits. An example lattice for the injection and extraction orbits is shown in Figure 6. Figure 7 plots the horizontal and vertical betatron tunes for all orbits, which corresponds to  $\sim 70^\circ$  phase advance per cell.

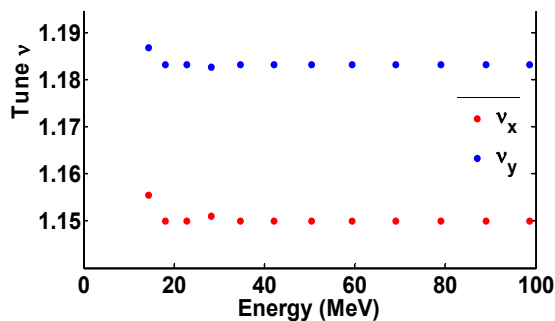


Figure 7: Betatron tunes vs energy for the SFC.

## CONCLUSION & FUTURE WORK

A method was developed for determining an optimum isochronous spiral orbit given choices for injection and extraction energy, maximum dipole field, and geometry and energy gain profile for slot-geometry cavities. A method was developed to optimize the focal lattice of F-D quadrupoles for desired phase advance/cell and to adjust the spiral lattice to maintain  $\sim$ constant horizontal and vertical betatron tunes for all orbits. The results of this optimization provide a framework in which we will next correct dispersion to near-zero at the cavity locations on all orbits and correct chromaticity.

In a companion paper [12] we report development of beam dynamics studies that take the optimization results reported here as the framework in which to study a progression of dynamical phenomena that will likely control the ultimate beam current that can be accelerated in an SFC: space charge lensing, synchro-betatron couplings, beam loading of the SRF cavities, and lateral propagation of wakefields between successive orbits in the cavities.

## REFERENCES

[1] S. Assadi *et al.*, ‘Strong-focusing cyclotron for high-current applications’, Proc. IPAC 2012, New Orleans, AIP Conference Proc. **1525**, 226-229 (2013).  
<http://accelconf.web.cern.ch/accelconf/ipac2012/papers/moppd033.pdf>

[2] P. McIntyre *et al.*, ‘Accelerator-driven subcritical fission to destroy transuranics in spent nuclear fuel and close the nuclear fuel cycle’, Proc. NAPAC2013, Pasadena.  
<http://accelconf.web.cern.ch/accelconf/pac2013/papers/mozab1.pdf>

[3] N. Pogue *et al.*, ‘Strong focusing cyclotron and its applications’, IEEE Trans. Appl. Superconduct. **25**, 3 (2015).  
<http://ieeexplore.ieee.org/stamp/stamp.jsp?arnumber=6965586>

[4] P. McIntyre *et al.*, ‘Accelerator-based neutron damage facility using LEDA’, *ibid.*  
<http://accelconf.web.cern.ch/accelconf/pac2013/papers/thoda2.pdf>

[5] N. Pogue *et al.*, ‘Superconducting RF cavity for high-current cyclotrons’, Proc. IPAC 2012, New Orleans, May 25-29, 2012.  
<http://accelconf.web.cern.ch/accelconf/ipac2012/papers/weppc063.pdf>

[6] J.N. Kellams *et al.*, ‘Superconducting sector dipole for a strong-focusing cyclotron’, Proc. Appl. Superconductivity Conf., Charleston, Aug. 5, 2014

[7] K. Melconian *et al.*, ‘Design of a MgB<sub>2</sub> beam transport channel for a strong-focusing cyclotron’, *ibid.*  
<http://ieeexplore.ieee.org/stamp/stamp.jsp?arnumber=6646204>

[8] S. Assadi *et al.*, ‘Nonlinear beam dynamics studies of high-intensity, high-brightness proton drivers’, Proc. IPAC2013, Pasadena.  
<http://accelconf.web.cern.ch/accelconf/pac2013/papers/tupac26.pdf>

[9] A. Cazan, P. Shutz, and U. Trinks, ‘Commissioning of the first separated orbit cyclotron TRITRON’, Proc. Int’l. Conf. on Cyclotrons and their Applications’, Caen (1998).  
<https://accelconf.web.cern.ch/accelconf/c98/papers/c-04.pdf>

[10] Wolfram Research, Inc., Mathematica, Version 10.1, Champaign, IL (2015).

[11] Methodical Accelerator Design (MADX):  
<http://mad.web.cern.ch/mad/>

[12] S. Assadi *et al.*, ‘Nonlinear beam dynamics studies of the next generation strong focusing cyclotrons as compact high brightness, low emittance drivers’, Proceedings of this conference.